euspen's 21st International Conference & Exhibition, Copenhagen, DK, June 2021
www.euspen.eu

Electrochemical micro-milling of niobium carbide (NbC) cermet with and without laser assistance

Muhammad Hazak Arshad[1,2], Krishna Kumar Saxena[1,2], Jun Qian[1,2], Dominiek Reynaerts[1,2]

[1]*Micro -& Precision Engineering Group, Department of Mechanical Engineering, KU Leuven, Belgium*

[2]*Member Flanders Make, Leuven, Belgium*

dominiek.reynaerts@kuleuven.be

Abstract

Niobium carbide (NbC) is a novel cermet material which is a potential material for cutting tool inserts and moulds as it has an excellent combination of hardness (comaparable to WC) and toughness. It is difficult to machine this multiphase material with conventional processes due to its high hardness and extreme mechanical properties. Therefore, the machinability of nickel bonded NbC cermet was evaluated experimentally with electrochemical micro-milling process, with and without laser assistance. Several channels were machined on the samples to study the process behaviour. The machined channels were observed under a confocal microscope and scanning electron microscope (SEM) along with analysis of machining current to provide insights on machinability of the NbC cermet. It was concluded that NbC can be effectively machined with electrochemical micromachining process. Additionally, laser assistance to electrochemical micromachining process enhances the electrochemical dissolution behaviour of the multiphase NbC cermet.

Keywords: Electrochemical micromachining, laser-electrochemical machining, hybrid machining, micro-milling.

1. Introduction

Cermets and cemented carbides are materials with carbides dissolved in a metal binder. Titanium (Ti) and tungsten (W) are most commonly used elements for metal carbides. The carbide particles impart hardness properties to the material and the metal binder is responsible for material toughness. This is a conflicting set of properties which gives cemented carbides numerous applications as the properties can be tailored to the required conditions. They are used mostly for cutting tools to machine materials with extreme mechanical properties. Cemented carbides are also used for heavy duty applications like drill bits due to high resistance to wear. Tungsten carbide is one of the most widely used cemented carbide. Cobalt (Co) on the other hand is the most common metallic binder due to its high wettability and solubility of carbide particles [1]. Pure niobium carbide (NbC) possesses a higher melting point (3608 ^{o}C) than WC (2870 ^{o}C) and almost half the density (7.8 gm/cm^3) of WC (15.7 gm/cm^3) along with high hardness up to 1960 (HV30). Due to these properties, NbC can be used to prepare cemented carbides by using less material mass for the same application ranges [2]. However, NbC has not been explored frequently as the main strengthening carbide phase but only as a grain growth inhibitor for WC based cemented carbides [3]. Recent research has shown NbC cermets to have similar or even higher wear resistance than WC cemented carbides [4] but better toughness and thermal shock resistance. Huang et al. [5],[6] recently fabricated NbC based cermets with various compositions and evaluated the material properties.

The extreme properties of NbC make it challenging to machine using conventional machining processes. Electrochemical micromachining (feature size < 2 mm) (ECM) process can be used for machining cemented carbides as this process is independent of material hardness. Eletcrochemical dissolution behaviour and mechanisms of tungsten carbides [7], [8] were reviewed to understand the dissolution behaviour of cermets. Since all the metals (Ti, W and Nb) belong to the same transition metals group, they should exhibit similar dissolution behaviour. It is relatively easier to machine TiC than WC due to lower standard electrode potential of Ti (-1.63 V) compared to W (0.1 V) using ECM. The strong passivation behaviour of WC limits ECM performance. WC passivates in sodium nitrate ($NaNO_3$) electrolyte and tungsten oxide adheres strongly to the workpiece surface which requires addition of a strong solvent, like sodium hydroxide (NaOH) in the salt-based electrolyte or reversal of the electrode polarities to generate NaOH in aqueous electrolytes [7]. Nb metal was also observed to easily passivate in alkaline medium [9]. Saxena et al. [10] recently explored machining of NbC and WC using ECM with and without laser assistance in an aqueous electrolyte solution of 25 g/l NaOH and 100 g/l $NaNO_3$. The results showed it was possible to machine NbC with ECM which exhibited high passivation and the cavity surface was more uniform with laser assistance.

This paper presents the machinability evaluation of NbC based cermets using electrochemical micromachinng with and without laser assistance. The micro-milled channels were observed under a scanning electron microscope (SEM) and confocal microscope to analyze the dissolution behaviour. Machining current was recorded to compare the effect of laser assistance on the kinetics of ECM process. Results show that NbC can be machined using ECM and that laser assistance improves the dissolution behaviour and enhances electrochemical dissolution kinetics for the parameters used in this study.

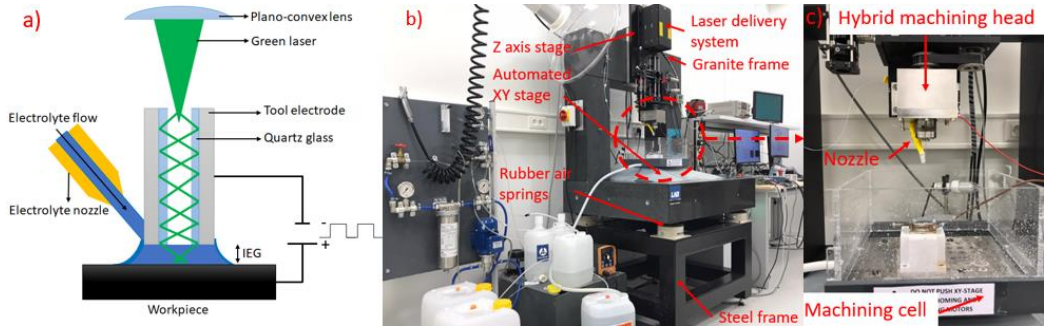

Figure 1: a) LECM process schematic, b) LECM experimental setup and c) Close-up of machining head

2. Experimentation

2.1. Hybrid laser-electrochemical micromachining setup

The tool based hybrid laser-electrochemical micromachining (LECM) setup developed by Saxena et al. [11] was used for the experiments with further hardware upgradation. The setup utilizes a tubular tool electrode (stainless steel tube with quartz glass capillary inside) of outer diameter 1.2 mm and inner diameter 0.35 mm, which can move below the workpiece surface. The updated setup shown in Figure 1, primarily consists of the LECM prototype, electrolyte flow system and machine control console. The LECM prototype itself consists of a machining cell, microsecond pulsed DC voltage source, nanosecond pulsed green laser delivery system (average power 30 W, max. pulse energy 180 µJ, max. pulse repetition rate 1500 kHz), hybrid machining head and a gantry type graphite-based machine frame. The hybrid machining head is supported by two angular contact ball bearings and can move along the z-axis with repeatability of ± 0.2 µm and resolution of 0.1 µm.

The XY stage (Standa® 8MTL120XY-Planar XY linear stage) uses direct drive technology to provide zero backlash motion with absolute accuracy of ± 0.5 µm after calibration and repeatability of ± 0.15 µm. The setup control is designed to simultaneously activate the XY stage and process energies. This is achieved by utilizing a LabVIEW® project with the NI® cRIO 9045 controller and LUMS software for the XY stage ACS drive. This control mechanism allows to machine multiple trajectories with accurate pulse control to switch the pulses OFF during non-machining movements of the XY stage. The hybrid machining head was modified to decouple the coaxial laser and electrolyte flow through the hollow tool electrode in order to reduce laser power loss. The electrolyte is supplied externally through a nozzle angled towards the tool electrode tip as shown in Figure 1(a), (c). About 23 % laser power loss (measured using Ophir® sensor) is observed with tool electrode of 45 mm length due to diffuse reflections within the tool because the stainless steel reflective surface is not perfectly smooth [10]. This attenuation further increases when using longer tool electrodes.

2.2. Samples preparation

Nickel bonded NbC cermet of composition NbC-12Ni-4Mo_2C-8WC was used for the electrochemical micro-milling experiments. The selected composition of nickel content gives a good balance of hardness, thermal shock resistance and toughness properties [2]. It has a hardness of 1300 (HV30) and fracture toughness of 9.2 MPa $m^{1/2}$ (K_{IC}). The samples were initially fabricated in the form of cylinders with complete densification through liquid phase sintering. The cylinders were cut into 3 mm thick discs using wire-electrical discharge machining (EDM). The surfaces of the sample discs were then grinded to obtain a smooth surface with a diamond resin grinding wheel of shape 1A1, grit size 46 µm and grit concentration 100.

2.3. Experimental procedure

Electrochemical micro-milling experiments were performed on NbC samples using the prototype hybrid laser-ECM setup. Channels were machined in order to study the process-material interaction. An aqueous 200 g/l $NaNO_3$ (conductivity 12.5 S/m at 16 ^{0}C) solution was used as an electrolyte to investigate ECM of NbC using an eco-friendly electrolyte and to avoid corrosion of precision machine components with electrolytes of higher or lower pH. The electrolyte was supplied using a solenoid metering pump connected to a flow nozzle with an exit diameter of 0.65 mm. The interelectrode gap (IEG) is set through an electrical touch mechanism. Several pilot-experiments were conducted to select a set of parameters as shown in Table 1. Three parallel channels of 8 mm length and 5 mm apart were machined for each machining condition namely, ECM and LECM. Experiments were done without tool rotation to minimize the influence of a variable (20 – 30) µm tool runout in order to achieve good repeatability of results. For laser assistance, the laser pulse energy was set to a low value of 8 µJ to prevent boiling of the electrolyte and material removal through laser ablation. The samples were cleaned in an ultrasonic bath of DI water (8 MΩ cm) for 20 mins after machining. The samples were weighed on a micro-balance from Mettler Toledo® XS105 with a readability of 10 µg and repeatability of 20 µg to calculate the material removal rate (MRR). Keyence® digital microscope was used to inspect the surface of the channels. SEM from Philips® XL30 FEG along with energy dispersive x-ray spectroscopy (EDX) was used to analyse the channels to understand the dissolution behaviour. The machining current was measured using a current acquisition module NI-9223 with a sample rate of 1 MHz.

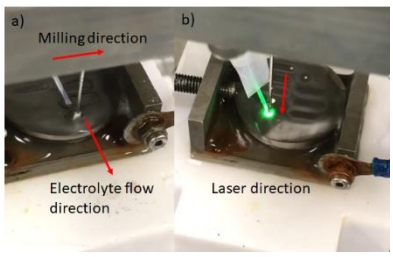

Figure 2: a) ECM and b) LECM

Table 1: Machining Parameters

Parameter	Value
Voltage	30 V
Electrolyte flow rate	0.75 ml/min
IEG	100 µm
Voltage pulse duty cycle	50 %
Voltage pulse width	10 µs
Milling feed rate	100 µm/s
Laser pulse energy	8 µJ
Laser pulse repetition rate	600 kHz,
Laser pulse width	10 ns

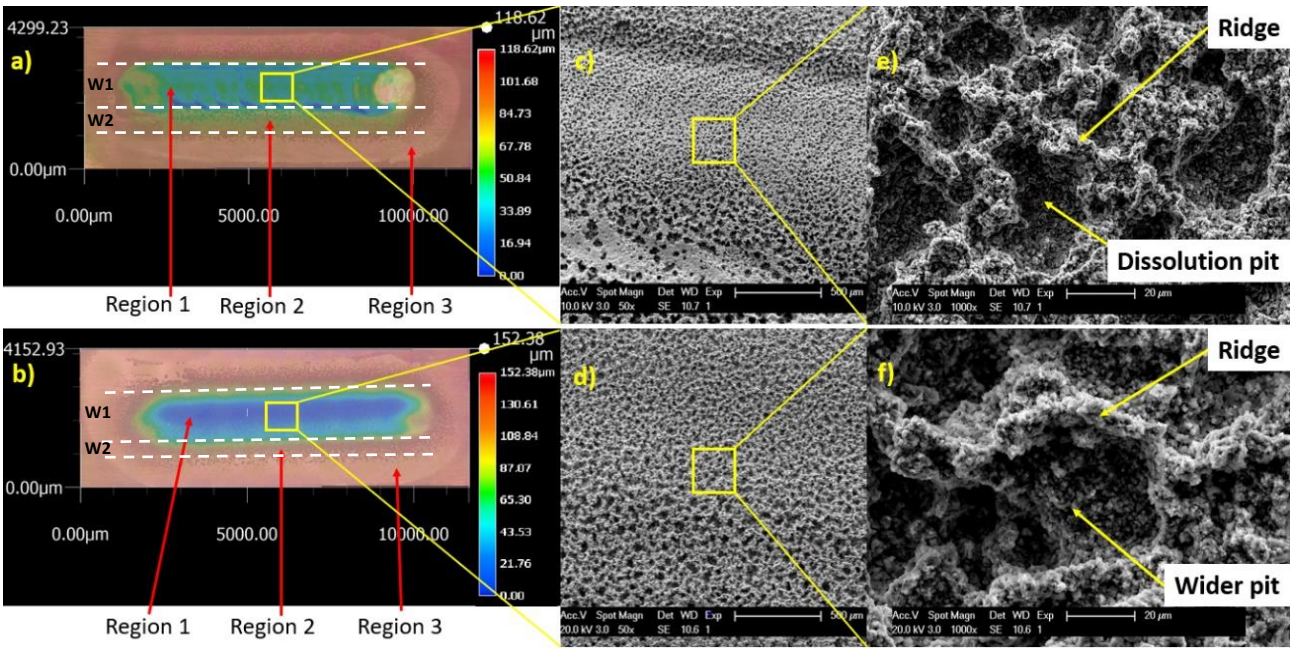

Figure 3: Confocal images [a) ECM and b) LECM], SEM images [c) ECM 50x, d) LECM 50x, e) ECM 1000x and f) LECM 1000x].

3. Results

3.1. Analysis of machined channels

The cleaned samples were first viewed under a Keyence® confocal microscope which revealed three distinct machining regions as shown in Figure 3(a), (b). The different regions exist due to the current density distribution along the width of the channel. The tool-electrode localizes the current density within the machining zone (of the order of tool-diameter) through the least resistance path for the flow of current in IEG. As the direction of electrolyte flow is inclined with respect to the machining zone to improve flushing of reaction by-products, it also distorts the current density distribution giving rise to the different machining regions [12], [13]. The channel surfaces were observed using SEM (as shown in Figure 3). The surface of region 1 is the primary machining region directly under the electrode which has a more uniform surface compared to the other regions due to the highest current density in this region. The edge of region 1 is quite distinct owing to the localization effect due to passivation in $NaNO_3$ electrolyte. The passivating layer on the channel walls restricts stray machining as the current is not strong enough to penetrate the layer along the width direction. As the channel width increases, the current density gradually decreases until it becomes too weak to effectively machine the material causing surface pitting which is the characteristic of region 2. Region 2 is much wider along the electrolyte flow direction which is expected due to directional flushing. Region 3 is merely surface passivation.

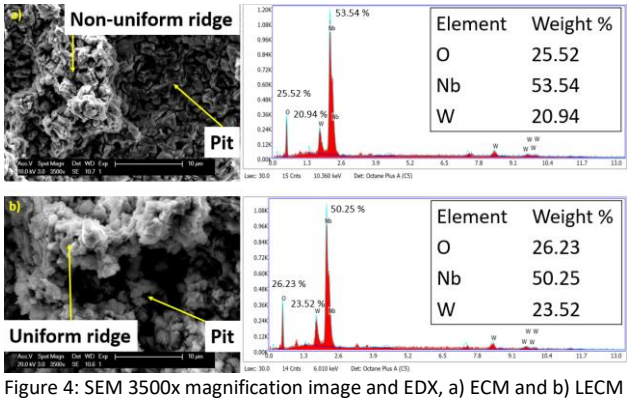

Figure 4: SEM 3500x magnification image and EDX, a) ECM and b) LECM

Comparison between the machined channels shows that region 1 (W1) is much wider and region of stray machining (region 2) (W2) is narrower in channel machined with LECM. The laser beam heats up the local electrolyte and workpiece surface increasing the electrolyte conductivity. This improves the reaction kinetics and transfer of current which escalates the material dissolution. The laser focus in the frontal gap weakens the passive layer in the depth direction and also facilitates trans-passive dissolution along the channel walls. For the channels in Figure 3(a),(b), region 2 width of channel machined with LECM decreased by 48.6 % (176.6 µm) as compared with region 2 width (343.4 µm) of channel machined with only ECM. For channel machined with LECM, region 1 width (2093.3 µm) increased by 30.3% as compared to region 1 width (1606.8 µm) of ECMed channel. Therefore, the channel width can be controlled more accurately with LECM due to reduction in stray machining. With LECM, average channel depth (131.62 µm ± 5.04) (distance between highest point and deepest point of channel) increased by 16.13 % as compared to channel depth (113.34 µm ± 32.69) with only ECM. The lower standard deviation with laser assistance signifies that material dissolves more uniformly and the process is more stable (for the set of parameters) than only ECM. Figure 3(c), (e) (ECM) and Figure 3(d), (f) (LECM) depict the central channel regions, showing that the material dissolution occurs in the form of dissolution pits. Also, the pits in the channels machined with LECM are much wider as compared to ECM alone. As the NbC cermet is a multiphase material, the different metal phases do not dissolve simultaneously due to difference in their standard electrode potentials [14]. The more reactive Nb and Ni contents are dissolved first. The non-conductive carbides fall out when the surrounding metal phases are dissolved. The pits are visibly wider with LECM due to the temperature induced increase in local current density which escalates the material dissolution. This is confirmed by the EDX results in Figure 4. The low percentage composition Mo_2C appears to have been completely removed in both machining conditions. The 3.29 wt.% decrease in Nb content with LECM is followed by an almost equal increase of 2.58 wt.% in W content. This indicates that the increase in current density increases Nb dissolution but it is possibly not high enough to enhance dissolution of the W content. The more uniform surface of the ridge (rich in oxides (passivation) and less reactive metal phases) with LECM indicates the existence of

trans-passive material removal due to heat induced conductivity increase which facilitates penetration of the passive layer.

The machined samples after cleaning were measured to observe the mass difference on a micro-scale to calculate the average MRR of all three channels for each machining condition. The average MRR was calculated by dividing the mass difference by the time needed to machine all three channels (240 s). Average MRR with LECM (0.15 mg) increased by 34.5 % when compared with only ECM (0.11 mg). This is due to the accelerated dissolution of NbC cermet with heat induced rise in local current density with LECM process.

3.2. Current measurements

The machining current was recorded throughout the channel machining at an acquisition rate of 1 MHz and logging rate of 1 Hz as the objective here is to compare the average current values and not instantaneous values. As a micro-second pulsed voltage source is used for ECM, Figure 5 shows the peak and root mean square (RMS) currents measured during the electrochemical micro-milling process. The increase in both the average peak (11.7 %) and average RMS (12.5 %) current values with LECM process validates the analogy that current density increases due to the heat by the laser beam which subsequently enhances dissolution rate of the NbC cermet. Another key observation is the curve fitted to the measured values clearly shows that the current fluctuation is much higher in ECM as compared to LECM. The current trend is almost straight in the case of LECM. This shows that the current during machining of channels with LECM fluctuates less in comparison with only ECM. Which implies that LECM is a more stable process for the selected experimentation parameters. Hence, LECM can machine multiphase NbC cermet more uniformly and is less affected by passivation and conductivity of different metal phases. When using solely ECM process, the machinig current fluctuates more because the process cannot penetrate the passive layer or dissolve less reactive metal phases, which decreases the current values when the machining zone becomes rich with these contents after the more reactive metal phases are dissolved.

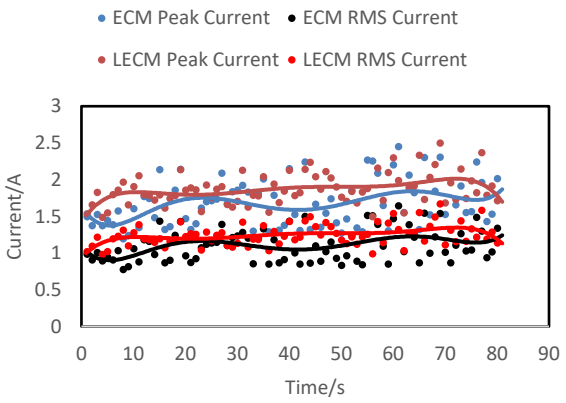

Figure 5: Measured machining current trends

4. Conclusion

The evaluation of machinability of NbC cermet using ECM with and without laser assistance is presented in this paper. Experimental investigations were done to study dissolution behaviour of the NbC cermet and to compare the process performance of ECM and LECM. Results indicate that the NbC cermet can be machined effectively with ECM. Comparative studies revealed that channels machined with LECM process had a more uniform surface, less stray machining, higher MRR and higher machining currents for the set of experimentation parameters due to increase in local current densities with laser assistance. The results achieved in this preliminary study of NbC machinability with ECM and LECM provide a basis to carry out more detailed experimental investigations of NbC machining using more parameter combinations and different machining conditions.

Acknowledgement

This work was supported by the FWO senior research project fundamental research (G099420N). The authors would like to thank Jide Han for assistance with SEM and the Department of Materials Engineering at KU Leuven for providing NbC samples.

References

[1] Mohammadpour M, Abachi P, Pourazarang K. Effect of cobalt replacement by nickel on functionally graded cemented carbonitrides. Int J Refract Met Hard Mater 2012;30:42–7. https://doi.org/10.1016/j.ijrmhm.2011.07.001.

[2] Zhou P, Song D, Wu H, Gao X, Nobufumi U, Katsunari O. Effect of Ni content on microstructure and properties of Co-based superalloys. Hangkong Cailiao Xuebao/Journal Aeronaut Mater 2019;39:73–80. https://doi.org/10.11868/j.issn.1005-5053.2019.000036.

[3] Huang SG, Liu RL, Li L, Van der Biest O, Vleugels J. NbC as grain growth inhibitor and carbide in WC-Co hardmetals. Int J Refract Met Hard Mater 2008;26:389–95. https://doi.org/10.1016/j.ijrmhm.2007.09.003.

[4] Woydt M, Mohrbacher H. The tribological and mechanical properties of niobium carbides (NbC) bonded with cobalt or Fe3Al. Wear 2014;321:1–7. https://doi.org/10.1016/j.wear.2014.09.007.

[5] Huang SG, Vleugels J, Altintas BT, Huang JH, Lauwers B, Qian J. Microstructure and mechanical properties of WC and Ti(C0.7N0.3) modified NbC solid solution cermets. J Alloys Compd 2021;850:156594. https://doi.org/10.1016/j.jallcom.2020.156594.

[6] Woydt M, Huang S, Cannizza E, Vleugels J, Mohrbacher H. Niobium carbide for machining and wear protection – Evolution of properties. Met Powder Rep 2019;74:82–9. https://doi.org/10.1016/j.mprp.2019.02.002.

[7] Natsu W, Kurahata D. Influence of ECM pulse conditions on WC alloy micro-pin fabrication. Procedia CIRP 2013;6:401–6. https://doi.org/10.1016/j.procir.2013.03.093.

[8] Schubert N, Schneider M, Michaelis A, Manko M, Lohrengel MM. Electrochemical machining of tungsten carbide. J Solid State Electrochem 2018;22:859–68. https://doi.org/10.1007/s10008-017-3823-9.

[9] Mickova I, Prusi A, Grcev T, Arsov L. Electrochemical passivation of niobium in KOH solutions. Croat Chem Acta 2006;79:527–32.

[10] Saxena KK, Qian J, Reynaerts D. A tool-based hybrid laser-electrochemical micromachining process: Experimental investigations and synergistic effects. Int J Mach Tools Manuf 2020;155:103569. https://doi.org/10.1016/j.ijmachtools.2020.103569.

[11] Saxena KK, Qian J, Reynaerts D. Development and investigations on a hybrid tooling concept for coaxial and concurrent application of electrochemical and laser micromachining processes. Precis Eng 2020;65:171–84. https://doi.org/10.1016/j.precisioneng.2020.05.014.

[12] Guo C, Qian J, Reynaerts D. Electrochemical Machining with Scanning Micro Electrochemical Flow Cell (SMEFC). J Mater Process Technol 2017;247:171–83. https://doi.org/10.1016/j.jmatprotec.2017.04.017.

[13] Liu G, Zhang Y, Natsu W. Influence of electrolyte flow mode on characteristics of electrochemical machining with electrolyte suction tool. Int J Mach Tools Manuf 2019;142:66–75. https://doi.org/10.1016/j.ijmachtools.2019.04.010.

[14] Zhu D, Yu L, Zhang R. Dissolution Effects with Different Microstructures of Inconel 718 on Surface Integrity in Electrochemical Machining. J Electrochem Soc 2018;165:E872–8. https://doi.org/10.1149/2.0761816jes.